CHAPTER 5

Computational investigation of the effect of W doping in MoS_2 lattice structure using DFT

5 Computational investigation of the effect of W doping in MoS_2 lattice structure using DFT

In chapters 3 and chapter 4, we have discussed the various properties like structural, optical, luminescence and photocatalysis of NPs of the ternary disulfide compound of Molybdenum and Tungsten along with MoS_2 and WS_2 NPs. In this chapter, we will very briefly discuss the electronic band structure of the ternary compound computationally by using DFT based software by constructing models of the ternary compound of Mo, W and S atoms.

5.1 Details of computational techniques employed

For the study of different properties of the mentioned compound, at first, we modeled a clone MoS_2. Then a periodic cell was constructed with eight molecules of MoS_2 from this clone. After that, we inserted W into it to make Mo_8WS_{16} system. As we were also interested to check how the system behaves when both Mo and W are in equal ratio, the content of W atom was increased and constructed $Mo_8W_8S_{16}$. All these structures were optimized and made free from any symmetry constraints. These structures are allowed to obtain minimum energy configuration by relaxing all the atoms in all directions.

We performed density functional calculations using GGA with PBE functional to describe the electron-electron exchange and correlation effects [1-5]. DFT equations were solved via PAW method using plane wave basis set as implemented in VASP and interfaced with MedeA technology platform [6]. The minimum energy state was computed by varying the internal position of atoms until the residual force was 0.01eV/Å. The electronic wave-functions were expanded using a plane-wave basis set with a cut-off energy of 480eV. The Brillouin-zone integration for geometry optimizations and electronic property calculations were performed by using a $3 \times 3 \times 5$ Monkhorst-Pack k-point grid for the structure [7]. Methfessel-Paxton type of smearing was used with smearing width of 0.2eV [8]. Real space projection operator was used as the system contained a large number of atoms.

5.2 Structural investigation

We investigated the changes brought out by the addition of W in the MoS_2 system. We optimized three systems (i) Mo_8S_{16} (ii) Mo_8WS_{16} and (iii) $Mo_8W_8S_{16}$. The systems Mo_8S_{16}, Mo_8WS_{16} and $Mo_8W_8S_{16}$ are shown in figure 5.1(a, b & c) respectively.

At first, we studied the structural changes that occurred in the ternary compound system as compared to Mo_8W_{16} system. Incorporation of W into Mo_8S_{16} i.e., Mo_8WS_{16} led to a more stable structure than Mo_8S_{16} whereas $Mo_8W_8S_{16}$ was observed to be the most stable structure as observed from DFT calculation. The volume of the cells (refer table 5.1) were affected by the combined effect of metal atoms in the ternary systems. The cell Mo_8S_{16} got compressed by the addition of W to it in the Mo_8WS_{16} system while $Mo_8W_8S_{16}$ got the largest volume. This is because when W atom was not introduced, spacing between nearby layers of MoS_2, called interlayer spacing, remained available. As a result of the addition of W atom in Mo_8WS_{16} structure, new bonds are formed among MoS_2 layers and

Table 5.1 Cell volume of minimized Mo_8S_{16}, Mo_8WS_{16}, and $Mo_8W_8S_{16}$ systems.

System	Cell volume ($Å^3$)
Mo_8S_{16}	520.123932
Mo_8WS_{16}	481.503624
$Mo_8W_8S_{16}$	721.114032

Table 5.2 Cell parameters of minimized Mo_8S_{16}, Mo_8WS_{16}, and $Mo_8W_8S_{16}$ systems.

Cell parameters	Mo_8S_{16}	Mo_8WS_{16}	$Mo_8W_8S_{16}$
a	14.828996	13.591858	14.652129
b	11.023554	11.078050	14.342715
c	6.364098	6.396561	8.728053
alpha	149.999733	150.004255	156.728332
beta	89.917164	90.034854	88.954058
gamma	90.443033	90.079907	88.755801

W atom which made the layers come closer and made the structure more compact. But when the number of W atom became more or equal to that of Mo atoms in the ternary model $Mo_8W_8S_{16}$, W formed new bonds in the layers and became part of it.

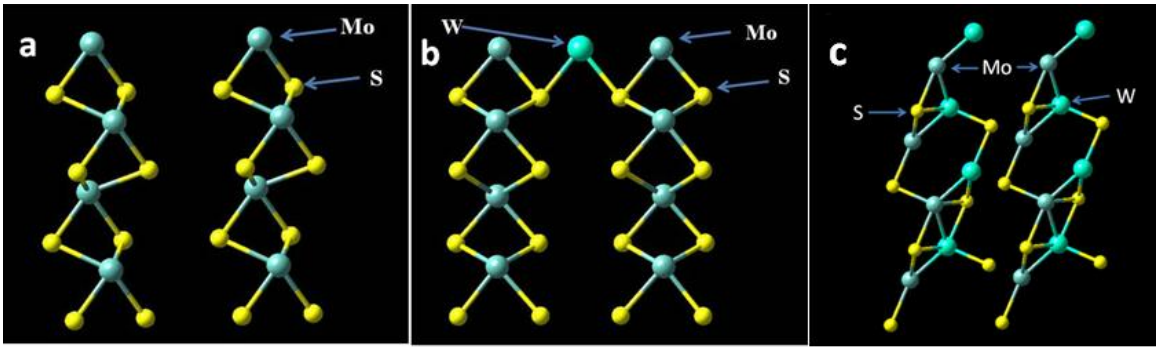

Figure 5.1 DFT model of (a) Mo_8S_{16}, (b) Mo_8WS_{16} and (c) $Mo_8W_8S_{16}$ systems.

Together with the interlayer spacing, the larger size of W atoms, which required more space, also resulted in the expansion of the system. The different cell parameters of the minimized structures are included in table 5.2.

5.3 Investigation of electronic band structure

In DFT, the electronic band structure of different materials is obtained by solving the basic Kohn-Sham (KS) equation by determining the effective potential [9]. The KS equation for non-interacting electrons in an effective potential V_{eff} (also known as KS potential) can be identified with an equation similar to Schrodinger equation like equation 5.1 which is given as

$$\left[-\frac{1}{2}\nabla^2 + V_{eff}\right]\psi_i = \varepsilon_i \psi_i \tag{5.1}$$

$$V_{eff} = V_{ext} + V_n + V_{xc} \tag{5.2}$$

where V_{ext} is the external potential, the second term V_n is the Coulomb potential due to charge distribution of electron density n and V_{xc} is the exchange-correlation potential. The energy BG E_g is related to the eigenenergy of equation 5.1 as

$$E_g = \varepsilon_{N+1}(N+1) - \varepsilon_N(N) \tag{5.3}$$

where ε_α is the highest occupied eigenenergy i.e the Fermi energy of α electron system. Sham et al. [9] and Kohn et al. [10] have discussed in details of basic KS equations and BG formulation. Different functionals in various approximations like LDA, GGA, meta GGA, hybrid functionals, etc. are adopted during DFT calculations via simulation for better accuracy [1-5, 9-15].

The band structures of the above-mentioned systems were investigated as reported in this section. Since Mo (Atomic number is 42 and electronic configuration is [Kr] $4d^5 5s^1$) is a d-bock element and W (Atomic number is 74 and electronic configuration is [Xe] $4f^{14} 5d^4 6s^2$) is an f-block element, their combined effect in the ternary system perturbed the band structure. In figure 5.2(a, b & c) the plots of band structure for the three mentioned systems are shown. We observed that in the model Mo_8W_{16} the CB minimum

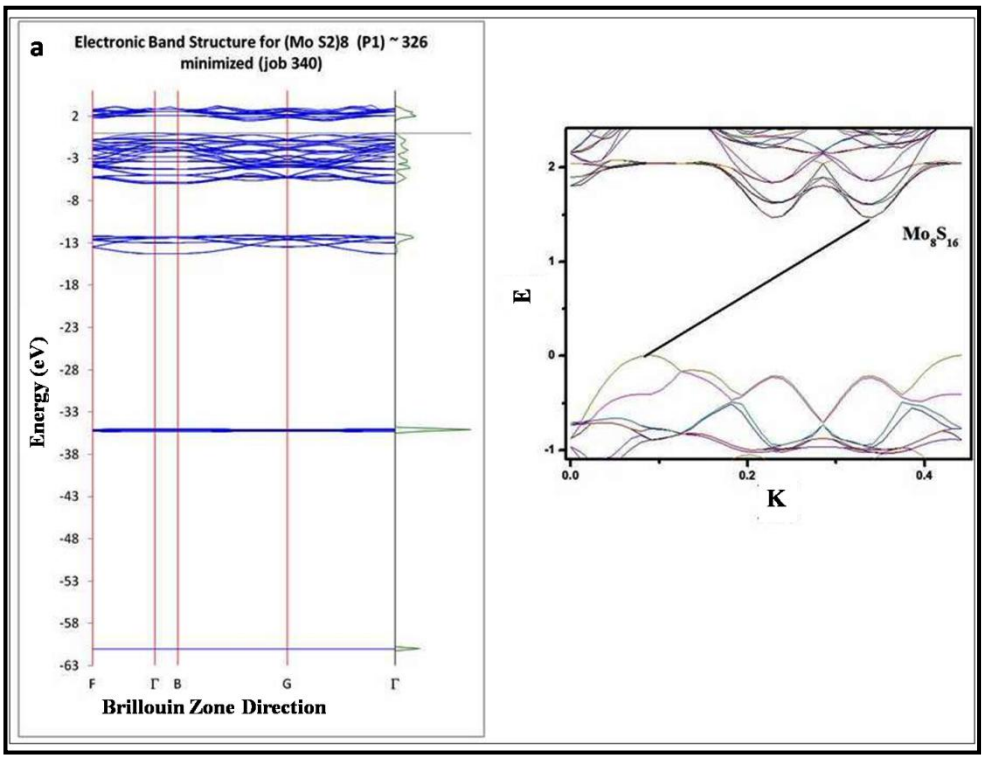

Figure 5.2 (a) Band structure plot of Mo_8S_{16}.

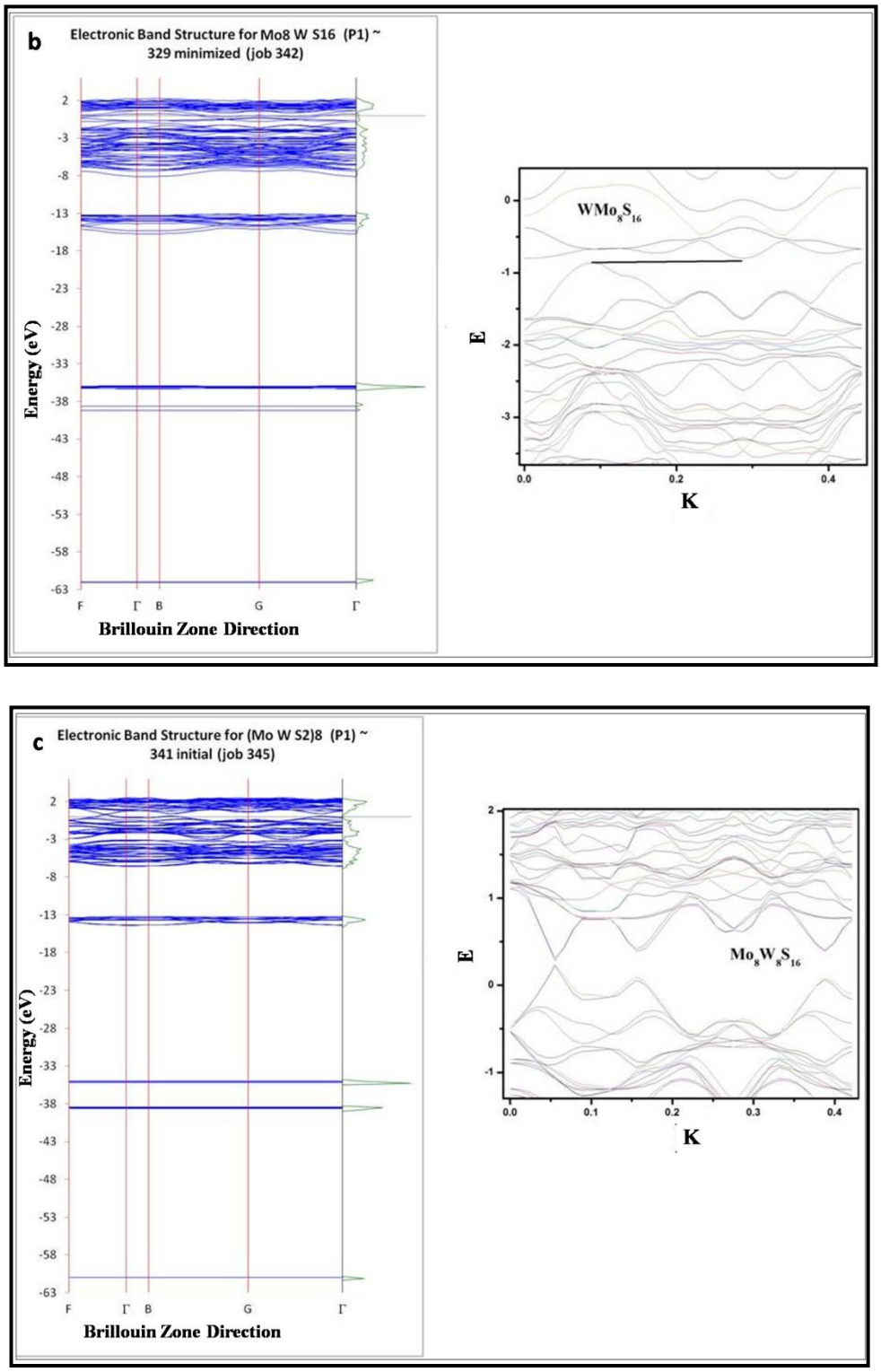

Figure 5.2 Band structure plot of (b) Mo_8WS_{16} and (c) $Mo_8W_8S_{16}$. The inset in each plot shows that the system transits from indirect to direct band gap system in $Mo_8W_8S_{16}$.

was not located at the same position of momentum (K value) of VB maximum in the E-K diagram. This type of band profile was also observed in the case of Mo_8WS_{16} system. But in the case of $Mo_8W_8S_{16}$ system, it was clearly seen that the VB maximum and CB minimum resided on the same K value point. The band structures thus depicted that the Mo_8S_{16} and Mo_8WS_{16} systems are indirect BG systems whereas $Mo_8W_8S_{16}$ has come out to be a direct BG system as envisioned in the inset of figure 5.2. However, the BG calculation error in DFT calculation is an inherent problem and is due to the lack of proper approximation; but from the band structure calculation in our study, we get the idea about the variation in the band structure of the above mentioned systems. It is found that insertion of W atom in the Mo_8S_{16} system changes the band structure drastically and allows the CB and VB to shift. The formation of new bonds might result in such shifting of bands which leads to direct nature of the BG in the $Mo_8W_8S_{16}$ system.

5.4 Investigation of the total density of states and partial density of states

In this section, we have investigated TDOS and PDOS of all the three model systems. Density of states (DOS) represents the number of particles (electrons or holes) for unit volume per unit energy for a given energy level and PDOS measures the relative contribution of individual atoms to the total DOS. On theoretical basis, the TDOS and PDOS can be determined by using formulae 5.4 and 5.5 as given below [16].

$$n(\varepsilon) = \frac{1}{(2\pi)^3} \int_{BZ} d^3k \delta[\varepsilon - \varepsilon_i(k)] \tag{5.4}$$

$$n_p(\varepsilon, r) = \frac{1}{(2\pi)^3} \int_{BZ} d^3k \delta[\varepsilon - \varepsilon_i(k)] |\psi_i(r)|^2 \tag{5.5}$$

where $\varepsilon_i(k)$ gives the electron energy at momentum k and ψ_i is the corresponding wave function. For solving the above equations the KS eigenvalue and wave function are calculated with a very dense k-point mesh. Thereafter, using a Gaussian or Lorentzian broadening function for the delta function the simulation is performed over the Brillouin zone. The ab-initio simulation technique for determining TDOS and PDOS has been discussed in detail by Kresse et al.[6].

The TDOS plot of all the system is shown in figure 5.3. The Fermi level is considered at 0 eV since we are more concerned about the states which are near the Fermi level. These

are the states which actively take part in optical transitions. The TDOS plot (black plot in figure 5.3) of the Mo_8S_{16} system shows a finite BG. The TDOS plot (red plot in figure 5.3) shows that the Mo_8WS_{16} have continuous states i.e it can be considered as a semi-metallic system. Also, the TDOS plot (blue plot in figure 5.3) of $Mo_8W_8S_{16}$ shows a finite but small BG which reveals the semiconductor nature of the system. Since the BG calculation via DFT is always less than the experimental value, so these states can be considered as sub states generated within the band gap of the system.

The PDOS for different states of Mo and S for the system Mo_8S_{16} system is shown in figure 5.4 (a & b). The PDOS of S i.e s and p states show that the s states hardly contribute in the nearby region of Fermi level whereas the existence of p states near the Fermi level is appreciable. In case of Mo the contribution of d states near Fermi level is more dominant than state s and p in band formation which is obvious because Mo is a d-block element. The PDOS of different states of Mo, W, and S of the system Mo_8WS_{16} is shown in figure 5.5 (a & b). The addition of W changes the scenario of Mo's d states near the Fermi level, in fact, these changes in Mo's d states turn this system into a semi-metallic system. The PDOS of various states of Mo, S and W in $Mo_8W_8S_{16}$ system is shown in figure 5.6 (a, b & c). The reason for considering this system was to investigate any effect when both W and Mo are in equal ratio. The PDOS pattern of Mo changed drastically compared to the last system and overall as well, the number of states near the Fermi level decreased. This signifies that bonding in this system are stable and the system overall is also stable which is in good agreement with the experimental observations.

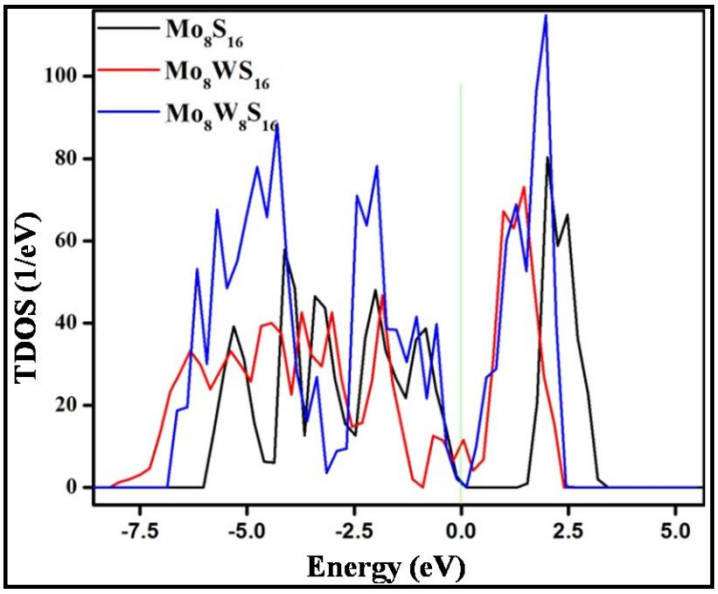

Figure 5.3 TDOS plot of Mo_8S_{16}, Mo_8WS_{16} and $Mo_8W_8S_{16}$.

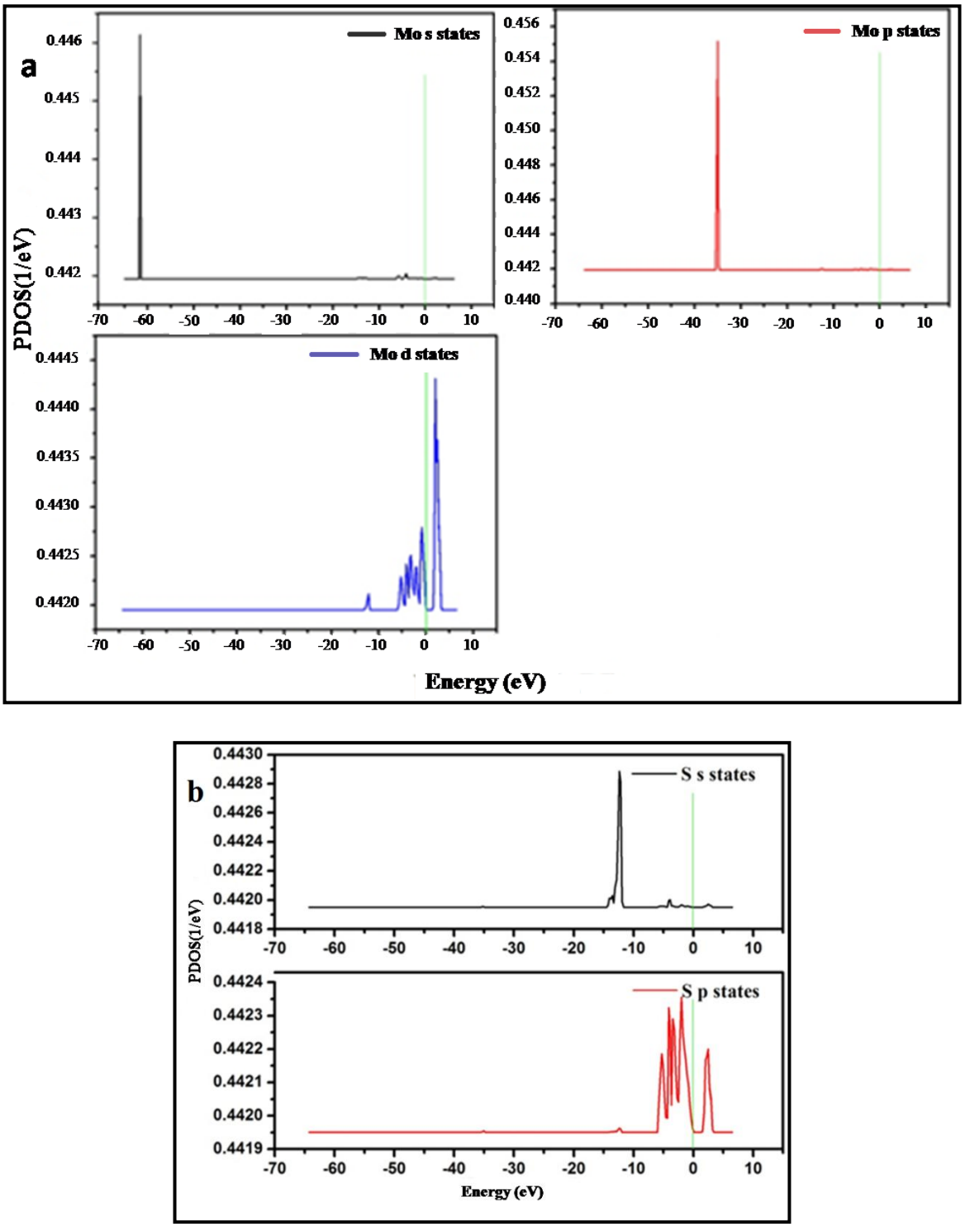

Figure 5.4 PDOS plot of Mo_8S_{16} showing (a) various states of Mo and (b) states of S.

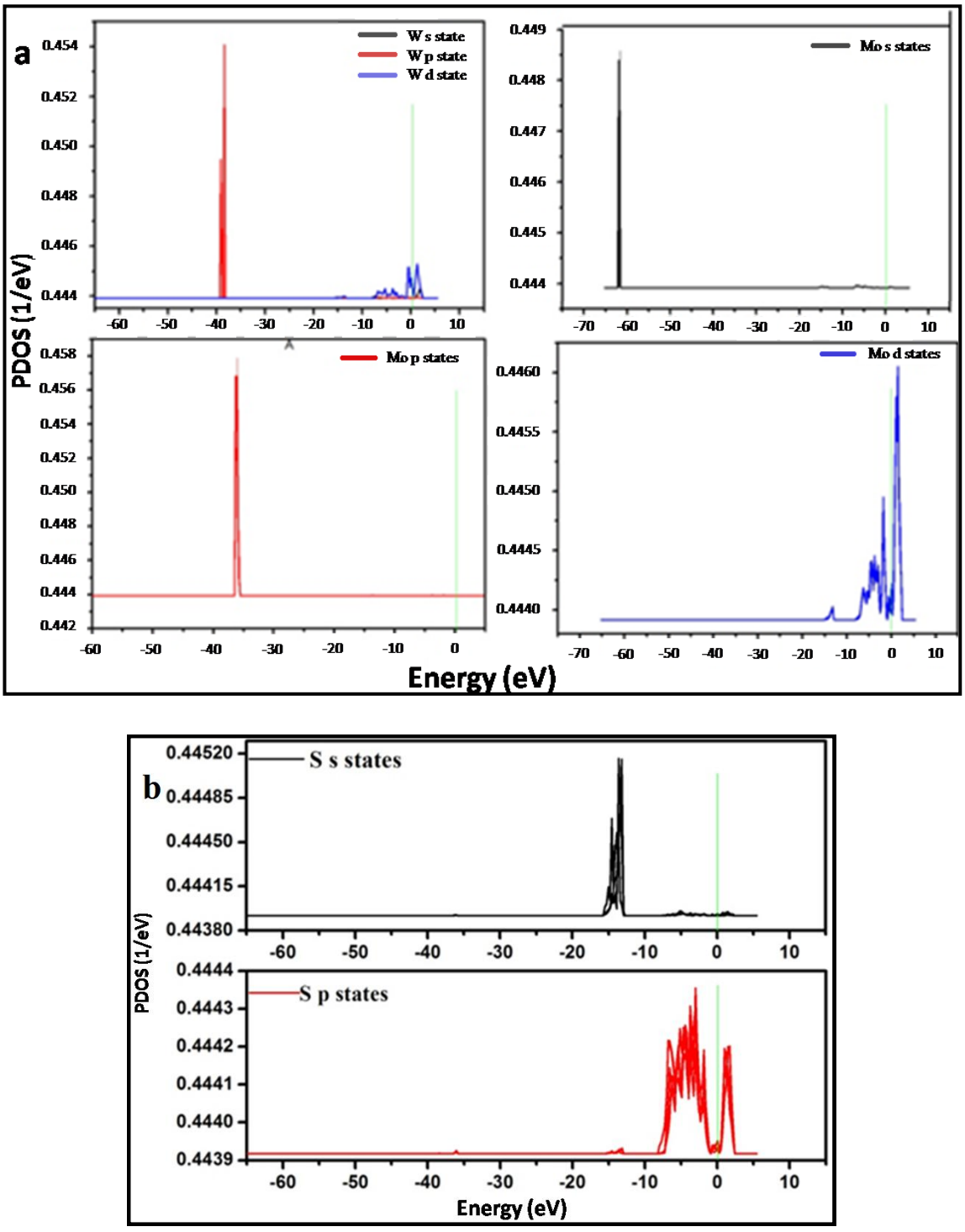

Figure 5.5 PDOS plot of Mo_8WS_{16} showing (a) various states of Mo and W, and (b) states of S.

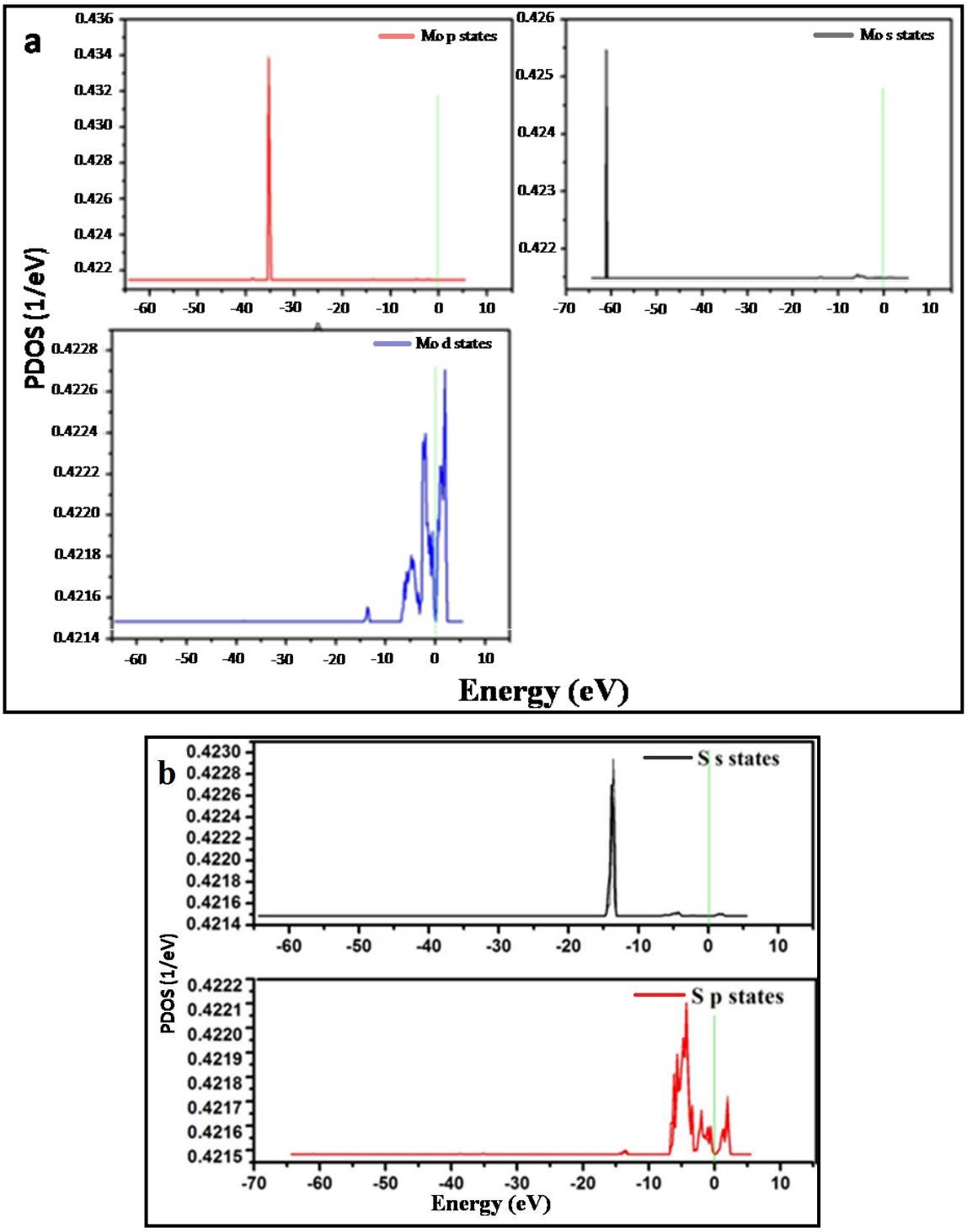

Figure 5.6 PDOS plot of $Mo_8W_8S_{16}$ showing (a) various states of Mo and (b) various states of S.

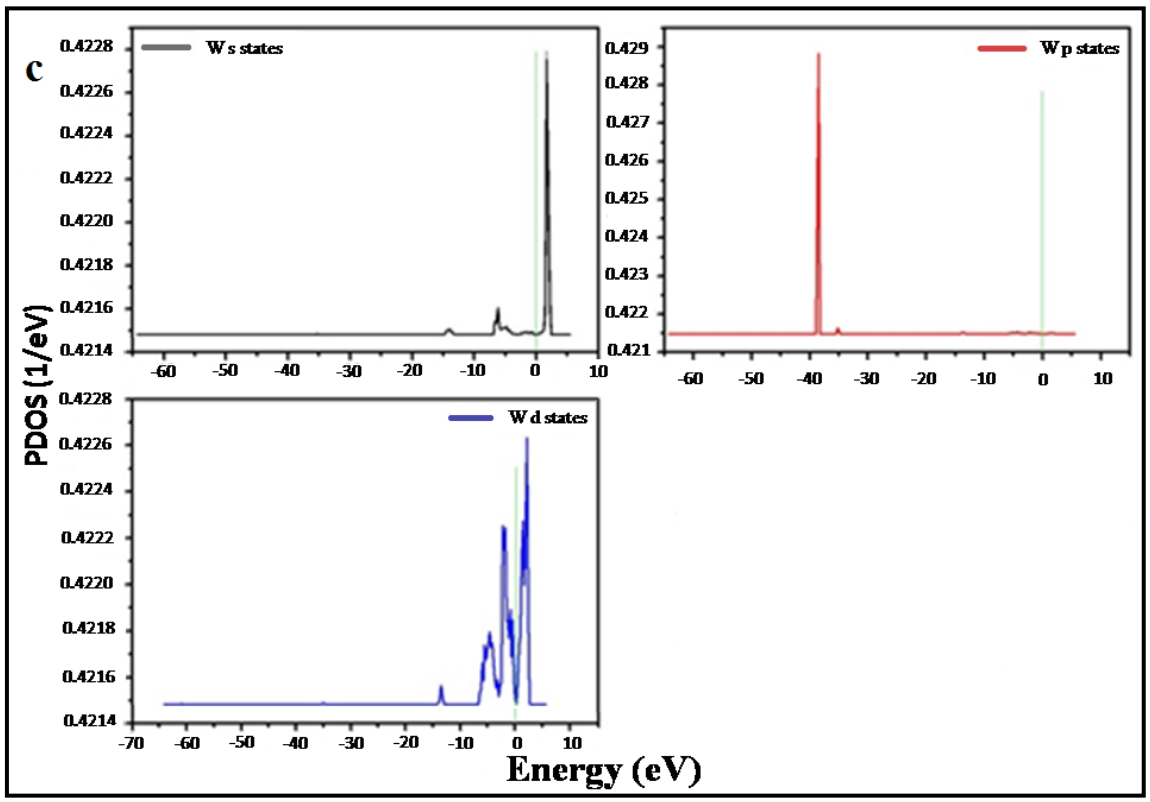

Figure 5.6 (c) PDOS plot of $Mo_8W_8S_{16}$ showing various states of W.

5.5 Conclusions

A computational investigation of the effect of W in the MoS_2 system using density functional theory (DFT) reveals that insertion of W in the MoS_2 system makes the ternary compound system more stable and it becomes most stable when Mo and W are in equal amount. Also, the DFT study concluded that the W insertion in the MoS_2 system leads the compound system to behave as direct BG semiconductor when W and Mo are equal in content and which agrees with the experimental results. The direct BG nature as determined with DFT simulation also gives good support to the results of enhancement in PL and photocatalytic activity of the compound MoWSulfide1 NPs as observed in chapter 3 and chapter 4.

[Note: This work is published in the Journal Bulletin of Materials Science.

Kalita, D., Chetia, L. Chetri, P., and Ahmed, G. A. Investigation of structural and luminescence properties of nanocrystalline Tungsten incorporated Molybdenum disulfide ternary compounds: An Experimental and DFT Study. *Bull. Mater. Sci.*, 42:134, 2019. DOI: 10.1007/s12034-019-1796-2]

References

[1] Harrison, N. M. An Introduction to Density Functional Theory. In Catlow, C. R. A., and Kotomin, E. A., editors, *Computational Materials Science*, pages 45-70, ISBN: 1586033352, IOS press, Netherlands, 2003.

[2] Ernzerhof, M. and Scuseria, G. E. Assessment of the Perdew-Burke-Ernzerhof exchange-correlation functional. *J. Chem. Phys.*, 110(11):5029-5036, 1999. DOI: 10.1063/1.478401

[3] Burke, K., Perdew, J. P., and Ernzerhof, M. Why the Generalized Gradient Approximation Works and How to Go Beyond It. *International Journal of Quantum Chemistry*, 61:287-293,1997.

[4] Perdew, J. P. Generalized gradient approximations for exchange and correlation: A look backward and forward. *Physica B*, 172: l-6, 1991.

[5] Perdew, J. P., Chevary, J. A., Vosko, S. H., Jackson, K. A., Pederson, M. R., and Singh, D. J., Fiolhais, C. Atoms, molecules, solids, and surfaces: Applications of the generalized gradient approximation for exchange and correlation. *PHYSICAL REVIEW B*, 46(11):6671-6687, 1992.

[6] Kresse, G., Marsman, M., and Furthmuller, J. VASP the GUIDE. Retrieved on 27.02.2015 from http://wolf.ifj.edu.pl/workshop/work2008/tutorial/vasp.pdf , 2005.

[7] Monkhorst, H. J. and Pack, J. D. Special points for Brillonin-zone integrations. *PHYSICAL REVIEW B*, 13(12):5188-5192,1976.

[8] Gordienko, A. B., and Filippov, S. I. A modified version of the methfessel-paxton Method. *Russian Physics Journal*, 52(7):668-673, 2009.

[9] Sham, L. J., and Schluter, M. Density-functional theory of the band gap. *PHYSICAL REVIEW B*, 32(6):3883-3889, 1985.

[10] Kohn, W. and Sham, L. J. Self-Consistent Equations Including Exchange and Correlation Effects. *PHYSICAL REVIEW*, 140(4A):A1133-A1138, 1965.

[11] Mendoza, M., Succi, S., and Herrmann, H. J. Kinetic Formulation of the Kohn-Sham Equations for ab initio Electronic Structure Calculations. *PRL*, 113:096402(5), 2014. DOI:10.1103/PhysRevLett.113.096402

[12] Kuisma, M., Ojanen, J., Enkovaara, J., and Rantala, T. T. Kohn-Sham potential with discontinuity for band gap materials. *PHYSICAL REVIEW B*, 82:115106(7), 2010. DOI: 10.1103/PhysRevB.82.115106

[13] Persson, C., and Ambrosch-Draxl C. A full-band FPLAPW+ k · p-method for solving the Kohn-Sham equation. *Computer Physics Communications*, 177:280–287, 2007. DOI:10.1016/j.cpc.2007.02.111

[14] Becke, A. D. Completely numerical calculations on diatomic molecules in the local-density approximation. *PHYSICAL REVIEW A*, 33(4):2786-2788, 1986.

[15] Perdew, J. P., Yang, W., Burke, K., Yang, Z., Gross, E. K.U., Scheffler, M., Scuseria, G. E., Henderson, T. M., Zhang, I. Y., Ruzsinszky, A., Peng, H., Sun, J., Trushin, E., and Gorling, A., Understanding Band Gaps of Solids in Generalized Kohn-Sham Theory. *PNAS*, 114(11):2801-2806, 2017. DOI:10.1073/pnas.1621352114

[16] Retrieved on 17.11.2018 from https://www.quora.com/What-is-projected-density-of-states.